Korean J Physiol Pharmacol 2023;27(2):187-196
https://doi.org/10.4196/kjpp.2023.27.2.187

KJPP

Original Article

Negative self-regulation of transient receptor potential canonical 4 by the specific interaction with phospholipase C-δ1

Juyeon Ko[#], Jinhyeong Kim[#], Jongyun Myeong, Misun Kwak, and Insuk So*

Department of Physiology, Seoul National University College of Medicine, Seoul 03080, Korea

ARTICLE INFO

Received November 26, 2022
Revised December 27, 2022
Accepted December 29, 2022

***Correspondence**
Insuk So
E-mail: insuk@snu.ac.kr

Key Words
Calcium
Fluorescence resonance energy transfer
Phosphatidylinositols
Phospholipase C delta
Transient receptor potential channels

[#]These authors contributed equally to this work.

ABSTRACT Transient receptor potential canonical (TRPC) channels are non-selective calcium-permeable cation channels. It is suggested that TRPC4β is regulated by phospholipase C (PLC) signaling and is especially maintained by phosphatidylinositol 4,5-bisphosphate (PIP_2). In this study, we present the regulation mechanism of the TRPC4 channel with PIP_2 hydrolysis which is mediated by a channel-bound PLCδ1 but not by the G_qPCR signaling pathway. Our electrophysiological recordings demonstrate that the Ca^{2+} *via* an open TRPC4 channel activates PLCδ1 in the physiological range, and it causes the decrease of current amplitude. The existence of PLCδ1 accelerated PIP_2 depletion when the channel was activated by an agonist. Interestingly, PLCδ1 mutants which have lost the ability to regulate PIP_2 level failed to reduce the TRPC4 current amplitude. Our results demonstrate that TRPC4 self-regulates its activity by allowing Ca^{2+} ions into the cell and promoting the PIP_2 hydrolyzing activity of PLCδ1.

INTRODUCTION

Transient receptor potential (TRP) channels are nonselective cation channels which are permeable to Ca^{2+}. Among TRP channels, this canonical family is composed of 7 types, and they are subdivided into two groups based on their amino acid sequence and structure; TRPC1, 4, 5 and TRPC3, 6, 7. Interestingly, TRPC4 is functionally analogous to TRPC5, but only TRPC5 shows constitutive activity even without stimulation. However, the mechanism that makes this difference still remains obscure. The activity of TRPC4 and TRPC5 are closely related to $G\alpha_q$-phospholipase C (PLC) signaling, and many studies also demonstrated the effect of downstream molecules on TRPC channels, which include PLC, phosphatidylinositol 4,5-biphosphate (PIP_2) [1-4], diacylglycerol (DAG) [5,6], protein kinase C (PKC) [7] and Ca^{2+}. We previously emphasized the self-limiting mechanism of $G\alpha_q$ pathway on channels where $G\alpha_q$ protein solely activates TRPC1/4 and TRPC1/5 channels, and PIP_2 depletion, PKC or Ca^{2+} inhibit them [8,9]. These data implicate that TRPCs are strongly activated by $G\alpha_q$, hence fast and tight regulation is necessary afterwards.

PLC is an enzyme that cleaves PIP_2 into inositol triphosphate (IP_3) and DAG. There are ten kinds of PLC isozymes that are largely classified into three families; β, γ, δ [10-13]. Among them, primordial PLCδ family has basic structure with the shortest length. The δ subtypes have about 10-fold higher sensitivity to calcium than the other isozyme [14,15]. The precise activation mechanism of PLCδ1 is not known, but it is expected that the Ca^{2+} concentration mainly controls their activity [16], and IP_3, the product of PIP_2 hydrolysis, is involved in its negative regulation [17].

PIP_2 is the most important component in TRPC channel's regulation as they are concerned with channel maintenance.

This is an Open Access article distributed under the terms of the Creative Commons Attribution Non-Commercial License, which permits unrestricted non-commercial use, distribution, and reproduction in any medium, provided the original work is properly cited. Copyright © Korean J Physiol Pharmacol, pISSN 1226-4512, eISSN 2093-3827

Author contributions: J. Ko designed the study, performed experiments, generated figures, analyzed data, and wrote the manuscript. J. Kim. generated figures and wrote the manuscript. J.M. performed confocal imaging, and M.K. performed Co-IP experiment. I.S. provided the overall experimental advice and coordinated the study. All authors reviewed the manuscript.

Other TRP channels are also known to be regulated by PIP_2 and the effect of PLCδ subtypes on this action has been proposed. PLCδ3 co-expression facilitated the desensitization of TRPV1 in oocytes [18], and subsequent PIP_2 reductions by PLCδ isoform promoted reduction in TRPM8 currents [19]. Thus, understanding the regulatory mechanism that alters TRPC activity related to the change in PIP_2 levels will provide insights on how channels are tightly regulated by PLC signaling, and how PIP_2 functions differently on TRPC channel functions.

In the present study, we set out to determine an effect of PLCδ on TRPC channel activity, and their working condition in this regulation. We verified that PLCδ1 directly interacts with TRPC4 but not with TRPC5, and it works as a key component of channel's negative feedback regulation. PLCδ1 is activated by the calcium *via* open TRPC4, and active PLCδ1 catalyzes the hydrolysis of PIP_2. These series of events reduced the current amplitude of TRPC4. We suggest the possibility that the involvement of PLCδ1 in channel regulation contribute to functional difference between TRPC4 and TRPC5.

METHODS

Cell culture and transfection

Human embryonic kidney (HEK)293 cells (ATCC) were maintained in Dulbecco's Modified Eagle's Medium (HyClone) supplemented with 10% heat-inactivated fetal bovine serum (Gibco), 100 U/ml penicillin, and 100 μg/ml streptomycin (HyClone) at 37˚C in a 5% CO_2 humidified incubator. Cells were seeded in glass bottom dish for imaging, 12-well plate for whole-cell patch clamp recordings, and 6-well plate for Western blot. The following day, transfection was carried out by using the FuGENE 6 Transfection Reagent (Promega) for patch clamp and imaging experiments, and Lipofectamine 2000 (Invitrogen) for western blotting according to the manufacturer's instructions. All experiments were performed 20–30 h after transfection. cDNA construct for mouse TRPC4 (GenBank ID: U50921.1, UniProt ID: Q9QUQ5-2) was kindly donated by Dr. V. Flockerzi and Dr. M. Schaefer, and that for human PLCδ1 (GenBank ID: U09117.1, UniProt ID: P51178-1) and human PLCδ3 (GenBank ID: BC072384.1, UniProt ID: Q8N3E9) by Dr. M. Zhu. The mutants of PLCδ1 were generated using a QuickChange site-directed mutagenesis kit (Agilent Technologies) following the manufacturer's protocol. The sequence was verified by sequencing.

Solutions and drugs

The recording pipette containing standard intracellular solution; 140 mM CsCl, 10 mM HEPES, 10 mM BAPTA, variable $CaCl_2$, 3 mM Mg-ATP, 0.2 mM Tris-GTP, was balanced to pH 7.3 with CsOH. The free Ca^{2+} concentration was calculated using CaBuf software (G.Droogmans). External solution was perfused constantly as follows; 135 mM NaCl, 5 mM KCl, 10 mM HEPES, 1 mM $MgCl_2$, 2 mM $CaCl_2$, 10 mM glucose, pH 7.4 with NaOH. Rapamycin was purchased from Sigma-Aldrich, and (-)-Englerin A (EA) was purchased from PhytoLab.

Electrophysiology

The cells were transferred onto a small chamber on the stage of an inverted microscope (IX70; Olympus), and attached to coverslip in the small chamber for 10 min prior to the recording. Transiently transfected cells were identified by their fluorescence tagging. Recording pipettes were pulled from glass capillaries (Harvard Apparatus) using puller (PC-10; Narishige). Whole-cell currents were recorded using Axopatch 200B amplifier (Molecular Devices) and Digidata 1550B interface (Molecular Devices). Experiments were performed at room temperature (18˚C-22˚C). The recording chamber was continuously perfused at a flow rate of 1–2 ml/min. Glass microelectrodes with 2–2.5 megaohms resistance were used to obtain gigaohm seals. The whole cell configuration was used to measure the TRPC4β channel currents in HEK293 cells. Voltage ramps ranging from +100 to –100 mV over a period of 500 ms were imposed every 10 sec with a holding membrane potential of –60 mV. pCLAMP v.10.2 (OriginLab) was used for data acquisition and the data were analyzed using the OriginPro 8 (OriginLab).

Image acquisition and FRET measurements

HEK293 cells were cultured in a 35-mm glass bottom dishes for imaging. For the confocal images, we used confocal laser scanning microscopy (LSM 710; Zeiss) equipped 63x oil objective lens. To obtain the FRET images, we used an inverted microscope (IX70; Olympus) equipped with 60x oil objective lens (UPlanSApo; Olympus). Each image was captured on an EMCCD camera (iXon3; Andor) and the light at 440 nm and 500 nm wavelengths was illuminated with LED light source (pE-2; CoolLED) under the control of MetaMorph7.6 software (Molecular Devices). Based on this imaging system, FRET measurements were made by the three-cube FRET method [20] (excitation, dichroic mirror, filter) *via* a fixed collimator. The illumination of specific wavelength and the emission filter were rotated sequentially, and the rotation period for each filter cube was ~0.5 sec. All of the images were obtained within a second. Every image was analyzed using MetaMorph 7.6 software (Molecular Devices).

FRET efficiency computation

We did FRET efficiency computation following methods in Ko *et al*. [3]. FRET Ratio (FR) is equal to the fractional increase in YFP emission due to FRET and calculated as:

$$FR = \frac{FA_D}{FA} = \frac{[S_{FRET}(DA) - R_{D1} \cdot SCFP(DA)]}{RA_1 \cdot [SYFP(DA) - R_{D2} \cdot SCFP(DA)}$$

Here, S_{CUBE}(SPECIMEN) denotes an intensity measurement, where CUBE indicates the filter cube (CFP, YFP, or FRET), and SPECIMEN indicates whether the cell is expressing the donor (D; ECFP), acceptor (A; EYFP), or both (DA). $R_{D1} = S_{FRET}(D)/(S_{CFP}(D)$. $R_{D2} = (S_{YFP}(D)/(S_{CFP}(D)$, and $R_{A1} = S_{FRET}(A)/S_{YFP}(A)$ are predetermined constants from measurements applied to single cells expressing only ECFP or EYFP-tagged molecules. Although three-cube FRET does not require that ECFP and EYFP fusion constructs preserve the spectral features of the unattached fluorophores, similar ratios and recorded spectra furnished two indications that the spectral features of the fluorophores were largely unperturbed by fusion. Since the FR relies on EYFP emission, EYFP should be attached to the presumed limiting moiety in a given interaction. Subsequent quantitative calculations based on FR relied on a presumed 1:1 interaction stoichiometry. The effective FRET efficiency (E_{EFF}) was determined as:

$$E_{EFF} = E \times A_b = (FR - 1)[E_{YFP}(440)/E_{CFP}(440)]$$

where E is the intrinsic FRET efficiency when fluorophore-tagged molecules are associated with each other, A_b is the fraction of EYFP-tagged molecules that are assoc0iated with ECFP-tagged molecules, and the bracketed term is the ratio of EYFP and ECFP molar extinction coefficients scaled for the FRET cube excitation filter [21]. We determined this ratio to be 0.094 based on maximal extinction coefficients for ECFP and EYFP and excitation spectra [22].

Western blotting, co-immunoprecipitation (Co-IP) analysis

We performed Western blotting following the methods in Kwak *et al*. [23], except with different antibodies. After transfection for 20–30 h, the cells were harvested as follows. Lysates were prepared in lysis buffer (0.5% Triton X-100, 120 mM NaCl, 50 mM HEPES, 2 mM $MgCl_2$, 2 mM EDTA, pH 7.5) by being passed through a 26-gauge needle ten to twenty times. Lysates were centrifuged at 13,000 × *g* for 10 min at 4˚C, and the protein concentration in the supernatants was determined. In the Co-IP experiments for detection of TRPC-PLCδ, 500 μl of cell lysates (500–1,000 μg) were incubated with 1 μg of anti-GFP antibody and 30 μl of protein G-agarose beads at 4˚C overnight with gentle rotation. After the beads were washed three times with wash buffer (0.1% Triton X-100), the precipitates were eluted with 30 μl of 2x Laemmli sample buffer and subjected to western blot analysis. The proteins extracted in sample buffer were loaded onto 8% Tris-glycine sodium dodecyl sulfate polyacrylamide gel electrophoresis (SDS-PAGE) gels. The proteins were transferred onto a nitrocellulose membrane. The following commercial antibodies were used: anti-GFP (A-11122; Thermo Fisher Scientific); anti-Flag (F3165; Sigma-Aldrich); and anti-β-tubulin (T-4026; Sigma-Aldrich).

Statistical analysis

All statistical analysis and graph generation were done with OriginPro8 (OriginLab). Results were compared using Student's t-test. A probability value (p) less than 0.05 was considered statistically significant. Data are presented as means ± SEM; $^*p < 0.05$, $^{**}p < 0.01$, $^{***}p < 0.001$.

RESULTS

TRPC4β directly interacts with PLCδ1

TRPC4β is functionally very comparable to TRPC5, but only TRPC5 shows constitutive activity even without the stimulation. Previously, we demonstrated that PIP_2 binds to TRPC4 and TRPC5 with different affinities [3]. Thus, we hypothesized that TRPC4 and TRPC5 channels have different mechanisms controlling the PIP_2 level. To support this hypothesis, we began studying the interaction of PLCδ enzyme with TRPC4 and TRPC5 channels. To identify the expression patterns, we performed fluorescence imaging experiments in a HEK293 cell line transiently co-transfected with ECFP tagged channel (TRPC4β or TRPC5) and EYFP tagged PLCδ (PLCδ1 or PLCδ3) enzyme. In the cases of expressing EYFP-PLCδ alone, PLCδ1 was expressed in the plasma membrane and was also distributed in the cytoplasm, and PLCδ3 was detected in the plasma membrane and the nuclear fraction (Supplementary Fig. 1). However, their expression pattern changed when they were co-expressed with TRPC4β. As shown in Fig. 1A, EYFP-PLCδ1 showed high fluorescence on the same location where TRPC4β-ECFP showed up as puncta on the membrane. The overlay image and line scan in this location showed an analogous fluorescence pattern (Fig. 1A *upper*). On the other hand, when TRPC4β-ECFP and EYFP-PLCδ3 were expressed together, PLCδ3 was observed mainly on the membrane, but it was not present in the TRPC4β expressing puncta region (Fig. 1A *bottom*). In other words, the distribution pattern of PLCδ3 was a total opposite to that of TRPC4β. We observed that TRPC5 did not colocalize with any of the PLCδ subtypes in the cells expressing ECFP-TRPC5 and EYFP-PLCδ1 or EYFP-PLCδ3 (Fig. 1C).

We used FRET imaging technique to determine whether colocalization of TRPC4β and PLCδ1 resulted from direct interaction or just close distances between these proteins. We used ECFP (donor)-TRPC ion channel and EYFP (acceptor)-PLCδ enzyme constructs to measure FRET efficiencies between them. As it was with the fluorescence imaging experiments, TRPC4β with PLCδ1 showed high FRET efficiency (Fig. 1B), but TRPC4β with PLCδ3, TRPC5 with PLCδ1 and TRPC5 with PLCδ3 showed low FRET

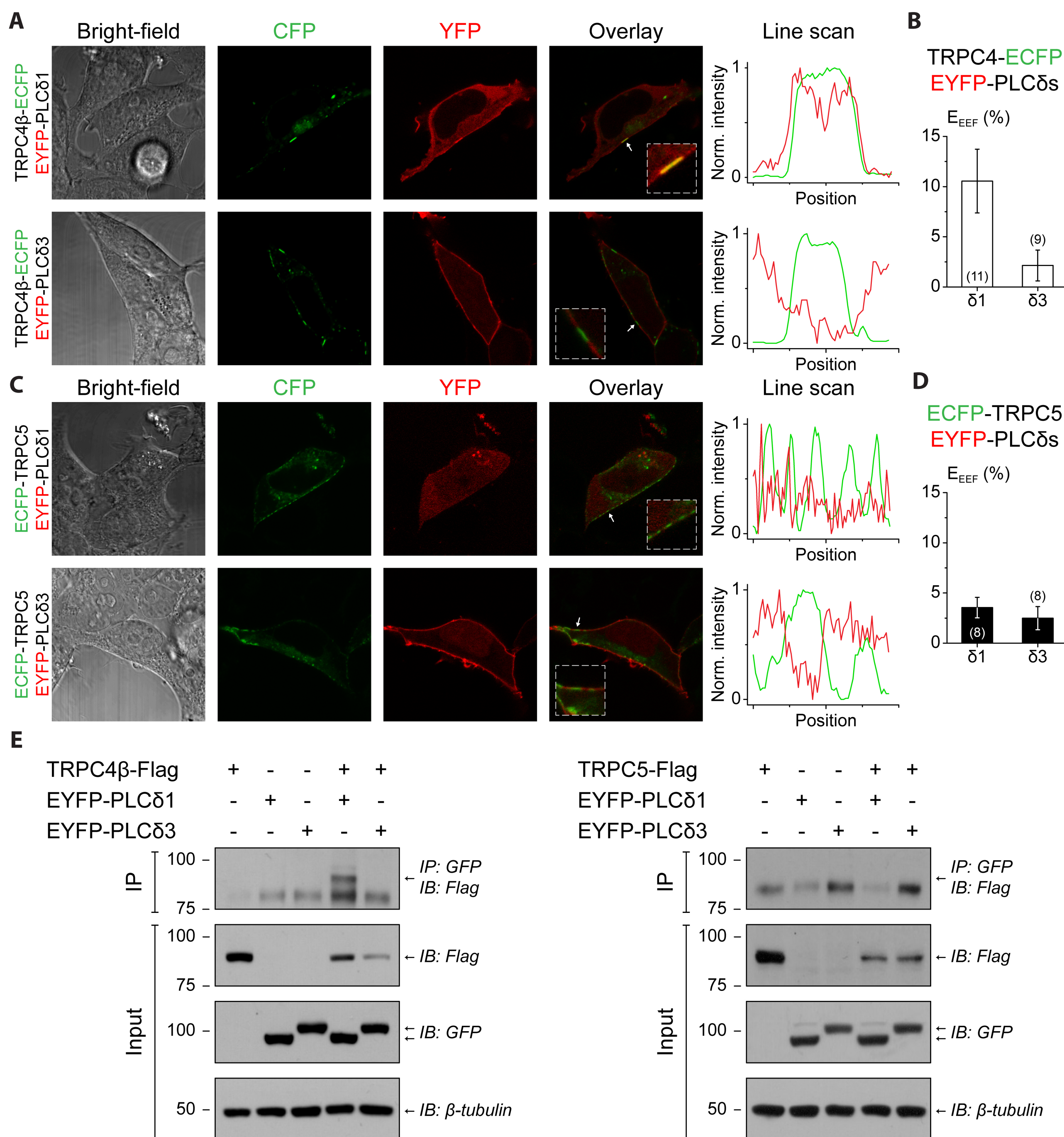

Fig. 1. TRPC4β and PLCδ1 colocalize together. (A, C) Localizations of TRPC channel and PLCδ enzyme. Upper panel: Channel with PLCδ1; Lower panel: Channel with PLCδ3. ECFP-tagged channel and EYFP-tagged PLCδ were co-expressed in HEK293 cells. The line scanned position is indicated by arrow in overlay images. Line scan graph shows TRPC4β colocalized with PLCδ1, but not with PLCδ3. Original magnification, ×63. (B, D) Summaries of FRET efficiency in the same expression conditions. The numbers in parentheses refer to cell numbers. (E) Representative blots of Co-IP experiments. HEK293 cells were co-expressed with Flag-tagged channel and EYFP-tagged PLCδ. Proteins from each condition were subjected to immunoprecipitation using anti-GFP antibody and probed with anti-Flag antibody. TRPC4β interacts with PLCδ1 directly but not with another subtype. TRPC5 interacts with neither. Data are expressed as mean ± SEM. TRPC, transient receptor potential canonical; PLC, phospholipase C; Co-IP, Co-immunoprecipitation.

efficiency (Fig. 1D).

As a final approach to identify the binding between TRPC and PLCδ, we expressed Flag tagged TRPC ion channel and EYFP tagged PLCδ enzyme and analyzed them *via* Co-IP. Protein was immunoprecipitated with anti-GFP antibody and then probed with anti-Flag antibody. The IP band was observed only in the cells expressing TRPC4β and PLCδ1, which indicates that only TRPC4β interacts with PLCδ1 (Fig. 1E).

PLCδ1 decreases TRPC4β currents amplitude and cytosolic Ca^{2+} determines the activity of PLCδ1

To determine the function of PLCδ1 on TRPC4β, we measured the changes in channel current. We used rapamycin-inducible system to translocate PLCδ1 to the membrane. HEK293 cells were transfected with CFP-FKBP-PLCδ1 and Lyn-FRB, and 50 nM of rapamycin was used, which is sufficient to translocate the PLCδ1 to the membrane (Fig. 2A). To investigate the changes in the TRPC4β current, we performed whole-cell patch clamp experiments with ramp pulse protocol from +100 to –100 mV every 10 sec in cells expressing TRPC4β, CFP-FKBP-PLCδ1, and Lyn-FRB. First, cells were treated with 50 nM rapamycin to translocate PLCδ1 with an efficient amount, then TRPC4β was stimulated by a channel agonist, EA (100 nM). In the cells not expressing Lyn-FRB, rapamycin did not show any current changes compared to basal current, and EA-evoked TRPC4β currents showed the characteristic double-rectifying current-voltage relationship (Fig. 2B). The presence of Lyn-FRB showed the characteristics of TRPC4β, however, the currents with EA stimulation were significantly decreased (Fig. 2C, D). Thus, these results suggest that PLCδ1 functions as a negative regulator of TRPC4β, reducing the current amplitudes.

We also investigated the Ca^{2+}-dependent effect of PLCδ1 on TRPC4β channel currents. TRPC channels are potentiated by intracellular calcium [24], and especially, Ca^{2+} is the main regulator of PLCδ1 activity [16]. Thus, we performed whole-cell patch clamp experiments by using different internal Ca^{2+} buffering solutions. We used 10 mM BAPTA in recording pipette to tightly buffer the concentration of free calcium to be 50, 100 and 500 nM. HEK293 cells were expressed with TRPC4β alone or together with PLCδ1, and channels were stimulated with 100 nM EA. Channel currents were recorded with ramp pulse protocol from +100 to –100 mV every 10 sec. With 50 nM $[Ca^{2+}]_i$ buffered internal solution, TRPC4β alone or TRPC4β and PLCδ1 expressing cells produced currents slowly after EA stimulation (Fig. 3A). In this condition, the presence of PLCδ1 did not significantly decrease the TRPC4β channel's peak current density (Fig. 3B). By increasing $[Ca^{2+}]_i$ to 100 nM, TRPC4β expressing cells showed relatively faster time course to reach the peak current (Fig. 3C). Notably, the EA-evoked current was significantly decreased in the cells expressing PLCδ1 together with TRPC4β (Fig. 3D). These aspects of decreased current in the cells expressing PLCδ1 were also observed in the experiments with 500 nM $[Ca^{2+}]_i$ pipette solutions (Fig. 3F). Interestingly, they showed robust current activation and desensitized quickly after reaching the peak current (Fig. 3E). Exceptionally, the time course of TRPC4 with or without PLCδ1 was different only in 100 nM calcium buffering condition. In the cells only expressing TRPC4β, higher internal calcium concentration potentiates channel to show a faster time course, and 500 nM $[Ca^{2+}]_i$ is sufficient to activate endogenous PLC to cause desensitization. PLCδ1 reduced the overall TRPC4β

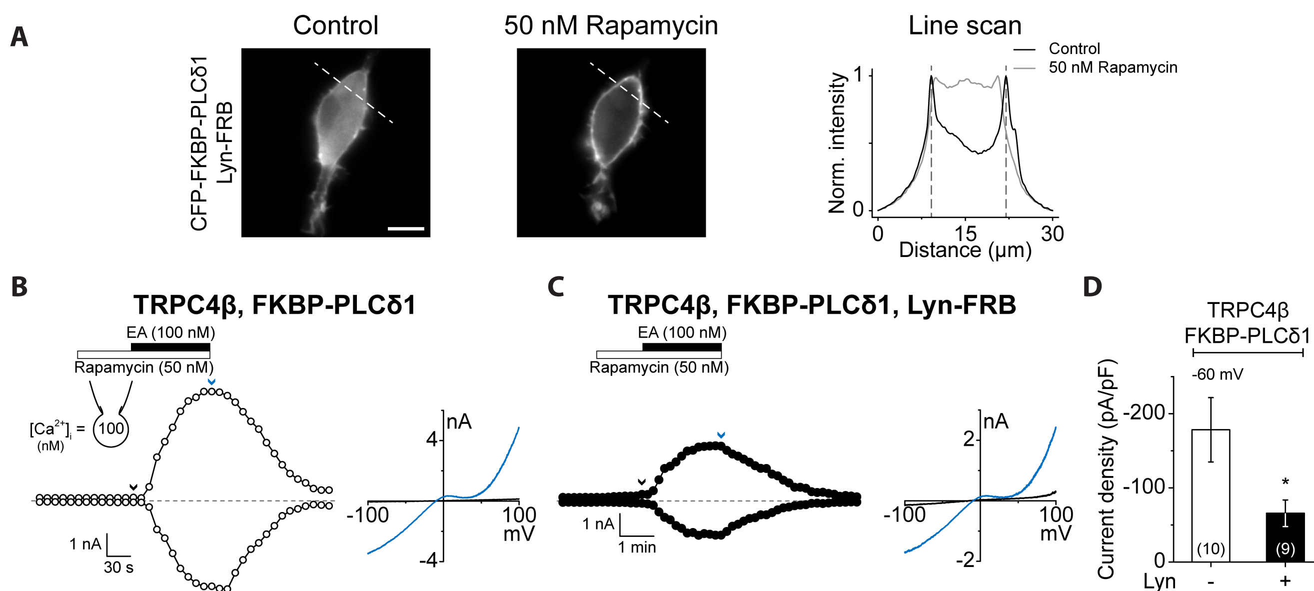

Fig. 2. PLCδ1 inhibits TRPC4β currents. (A) Rapamycin-induced translocation of CFP-FKBP-PLCδ1 to the plasma membrane. CFP-FKBP-PLCδ1 and Lyn-FRB were co-expressed in HEK293 cells, and 50 nM rapamycin was used. The line scanned region is indicated by dashed line. Scale bars, 10 μm. (B, C) Representative whole-cell current recordings of HEK293 cells co-expressed with TRPC4β, FKBP-PLCδ1 in the absence (B) or presence of Lyn-FRB (C). Left panel: Time course of currents at ±100 mV every 10 sec; Right panel: I-V relationship for selected time points. Stippled lines indicate zero currents. Applications of 50 nM rapamycin and 100 nM (-)-Englerin A (EA) are indicated. The pipette solution contained 100 nM free Ca^{2+}. (D) Summaries of peak current densities at –60 mV induced by rapamycin and EA. Rapamycin-induced PLCδ1 translocation to plasma membrane significantly reduced TRPC4β currents. Data are expressed as mean ± SEM. TRPC, transient receptor potential canonical; PLC, phospholipase C. *$p < 0.05$ by t-test. The numbers in parentheses refer to cell numbers.

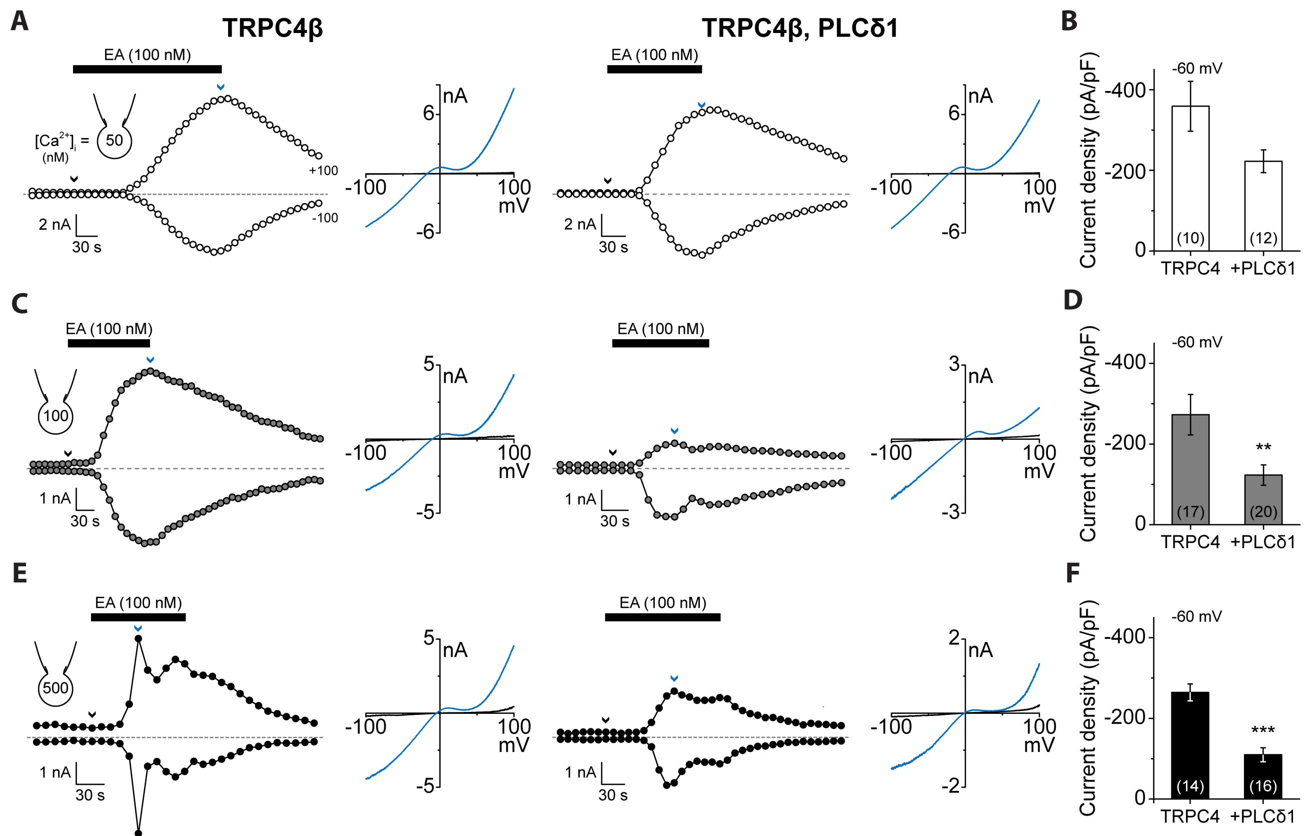

Fig. 3. Ca^{2+}-dependent activation of PLCδ1 occurs in physiological intracellular calcium range. (A, C, E) Representative whole-cell current recordings of HEK293 cells co-expressed with TRPC4β in the absence or presence of PLCδ1 using 50 nM (A), 100 nM (C), and 500 nM (E) free Ca^{2+} recording pipette solutions. Left panel: Time course of currents at ±100 mV every 10 sec; Left panel: I-V relationship for selected time points. Stippled lines indicate zero currents. Applications of 100 nM (-)-Englerin A (EA) are indicated. (B, D, F) Summaries of peak current densities at –60 mV induced by EA. The PLCδ1 inhibited TRPC4 currents when using 100 nM and 500 nM $[Ca^{2+}]_i$ recording solutions. Data are expressed as mean ± SEM. TRPC, transient receptor potential canonical; PLC, phospholipase C. **p < 0.01, ***p < 0.001 by t-test. The numbers in parentheses refer to cell numbers.

currents in 100 nM and 500 nM free Ca^{2+}. Therefore, we suggest that physiological calcium concentration is sufficient to activate PLCδ1 after channel stimulation, and the activity of PLCδ1 is tightly regulated in a calcium dependent manner.

TRPC4β-mediated increase in intracellular Ca^{2+} concentration activates PLCδ1, and it accelerates PIP_2 depletion

PLC is an enzyme that cleaves phospholipids in a Ca^{2+}-dependent manner. TRPC4 channel is a nonselective cation channel which is permeable to calcium as well as monovalent cations. Therefore, Ca^{2+} influx-induced by TRPC4β activation may act as a stimulator of PLCδ1. To identify the activity of PLC, we used PH-domain of PLCδ1 as a PIP_2 sensor to monitor the PIP_2 changes. We co-transfected TRPC4β, PLCδ1, and CFP-tagged PH domain in HEK293 cells, and TRPC4β was stimulated by 100 nM EA. At first, CFP-PH was observed on the membrane, and line scan showed dense fluorescence intensity in the membrane before channel stimulation. In the cells expressing TRPC4β without PLCδ1, CFP-PH still showed similar intensity in the membrane even after 30 sec of EA stimulation and PIP_2 started to deplete after 60 sec (Fig. 4A). On the other hand, TRPC4β and PLCδ1 co-expressed cells showed relatively faster PIP_2 depletion from membrane. In these cells, 30 sec of EA stimulation was enough to deplete the membrane PIP_2 (Fig. 4B). These results suggest that calcium influx *via* TRPC4β activates PLCδ1, and it causes the acceleration of PIP_2 depletion.

As a final approach, we evaluated the effect of PLCδ1 on TRPC4β. We used two mutant forms of PLCδ1 (Supplementary Fig. 2). The first mutant is PLCδ1 (K30A/K32A) which interrupted the PIP_2 binding, as Lys30 and Lys32 residues are located in the PH-domain [25]. And the second one is PLCδ1 (H311A) which shows abolished phospholipase activity since His311 residue is located in the X-region of catalytic domain (Fig. 5C) [26]. We measured TRPC4β currents in the cells expressing TRPC4β and PLCδ1 (K30A/K32A) or PLCδ1 (H311A) mutant, respectively. Whole-cell patch clamp experiments were performed using the same protocol as mentioned before and the intracellular free calcium concentration was buffered to be 100 nM. In the cells

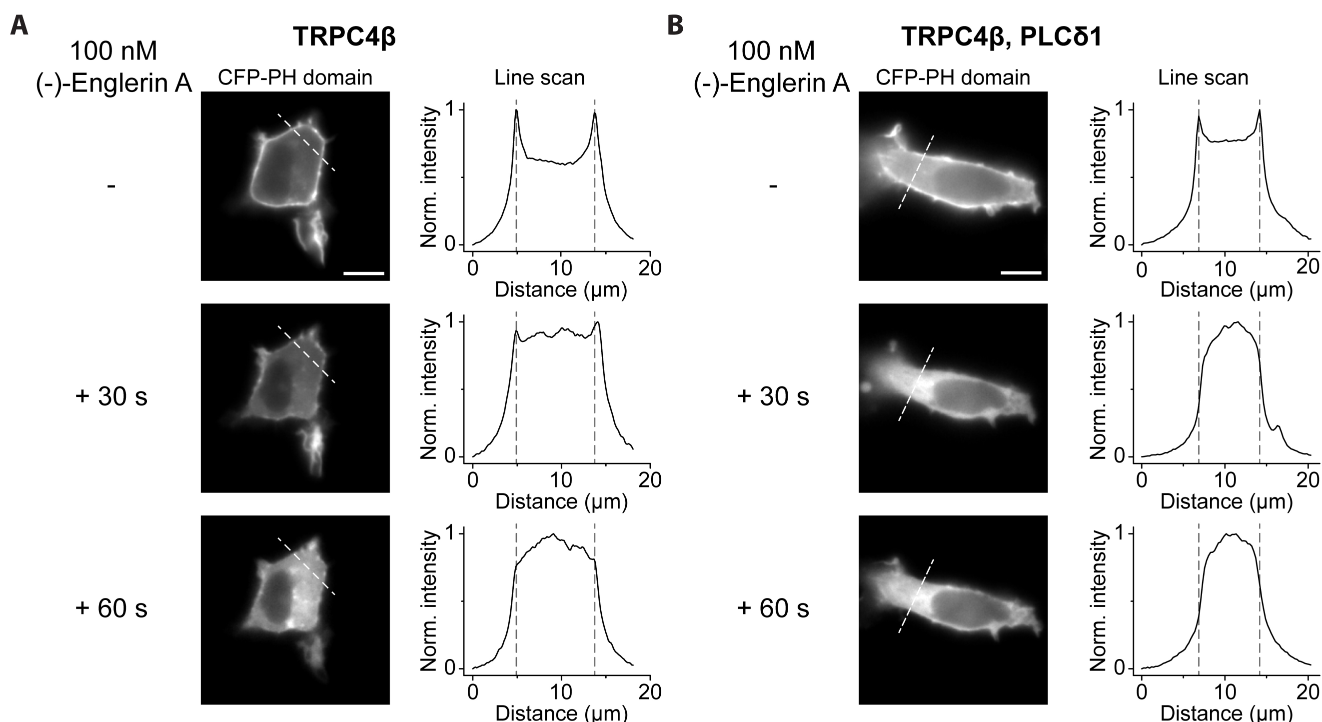

Fig. 4. Channel calcium-activated PLCδ1 accelerates PIP_2 depletion. (A, B) PIP_2 depletion from plasma membrane to cytosol after (-)-Englerin A stimulation. Imaging was performed in the cells expressing TRPC4β and CFP-PH domain in the absence (A) or presence of PLCδ1 (B). PIP_2 changes are monitored by CFP-PH domain. Left panel: Images of CFP-PH domain for selected time points; Right panel: Line scan graph of each image. The line scanned regions are indicated by dashed line. Scale bars, 10 μm. TRPC, transient receptor potential canonical; PLC, phospholipase C; PIP_2, phosphatidylinositol 4,5-bisphosphate.

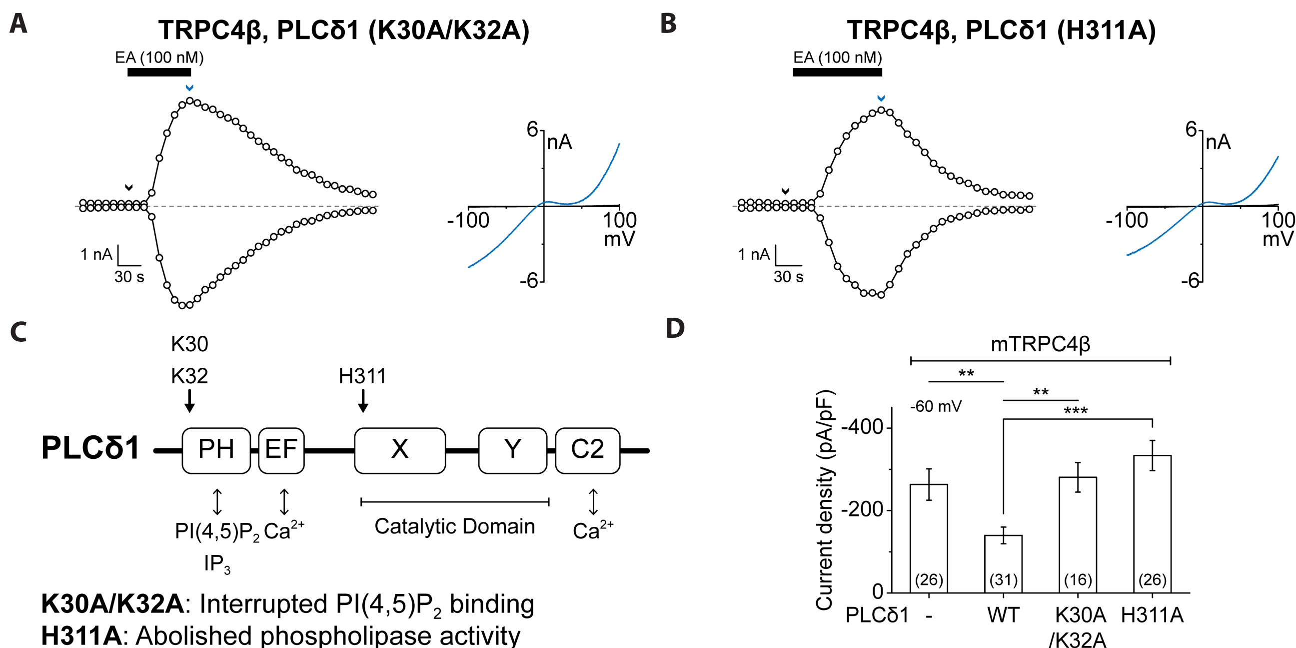

Fig. 5. Nonfunctional PLCδ1 mutants on PIP_2 level have no effect on TRPC4 currents. (A) Representative whole cell current recordings of HEK293 cells co-expressed with TRPC4β and PLCδ1 (K30A/K32A) (A) or PLCδ1 (H311A) (B). Left panel: Time course of currents at ±100 mV every 10 sec; Right panel: I-V relationship for selected time points. Stippled lines indicate zero currents. Application of 100 nM (-)-Englerin A (EA) are indicated. The pipette solution contained 100 nM free Ca^{2+}. (C) Schematization of PLCδ1. The mutation sites are indicated with arrow. (D) Summaries of peak current densities at –60 mV induced by EA. PLCδ1 mutants had no effect on TRPC4β currents as the PLCδ1 non-expressing cells. Data are expressed as mean ± SEM. TRPC, transient receptor potential canonical; PLC, phospholipase C. **$p < 0.01$, ***$p < 0.001$ by t-test. The numbers in parentheses refer to cell numbers.

expressing both mutants, the TRPC4β currents showed a similar time course as it would with cells expressing TRPC4β alone (Fig. 5A, B). Furthermore, EA-evoked currents in the cells expressing PLCδ1 (K30A/K32A) and PLCδ1 (H311A) with TRPC4β were significantly higher than in the cells expressing wild type PLCδ1, similar to the case when TRPC4β was expressed alone (Fig. 5D). In other words, PLCδ1 mutants which cannot regulate PIP_2 levels did not have any effect on the TRPC4β activity. Therefore, these results suggest that TRPC4β-bound PLCδ1 regulates PIP_2 level to decrease TRPC4β currents.

DISCUSSION

Activity of TRPC4 ion channel is closely controlled by PIP_2. In this study, we found that PLCδ1 binds to TRPC4 and contribute to channel regulation. The conclusions of this study are as follows: 1. TRPC4 directly interacts with PLCδ1, but TRPC5 has no interaction with any PLCδ subtypes, 2. PLCδ1 causes inhibition of TRPC4 currents in a calcium dependent manner, 3. TRPC4-bound PLCδ1 responds to the calcium influx by the channel, which in turn depletes PIP_2. Altogether, we propose a negative feedback regulation of TRPC4 by PLCδ1 in a Ca^{2+} and PIP_2 dependent manner.

Previously, we suggested that $G\alpha_q$-PLC pathway has a self-limiting activation on TRPC channels. The $G\alpha_q$ protein strongly activates TRPC heteromeric channels [8], and sequential events such as PIP_2 depletion, PKC activation, and Ca^{2+} increase result in channel inhibition [9]. We emphasized several times that regulation of PIP_2 level is the most important factor as they are a requisite for channel activity. Accordingly, this important role of PLC and PIP_2 on TRPC4 channel is not surprising. Several TRP channels are also known to be regulated *via* signaling cascade including PLC and PIP_2. For instance, PLC-mediated PIP_2 decrease is shown to be involved in the desensitization of TRPM4, 5, and 8, hence PIP_2 appears to play a key role and ever-present regulator of TRPM channels [19,27-29]. Furthermore, TRPM8 neurons express Ca^{2+}-sensitive PLCδ isozymes [30], and *in vivo* data showed that the activity is regulated by PLCδ4 [31]. Also, it is suggested that PIP_2 is necessary for the normal function of TRPV1 channel. In this context, the desensitization of the TRPV1 currents is accelerated and eventually completely suppressed when PLCδ3 is expressed together, and even such desensitization disappeared in PLCδ4-/- [32]. Based on the followings, we have studied the effect of PLC with δ subtype, which is most sensitive to Ca^{2+} *versus* other PLC subfamilies. Here, we provide an evidence that PLCδ1 directly interact with TRPC4β based on the results of FRET and Co-IP experiments (Fig. 1). The inclusion of PLCδ1 in regulation of TRPC4β channel activity has been reported as an underlying concept of inhibitory PIP_2. They suggested that TRPC4β activity was affected by PLCδ1 in preference to PLCδ3, and our data are consistent with this result that it might be from their direct interaction.

The direct interaction between TRPC4β and PLCδ1 also appeared clearly in expression patterns. PLCδ1 is expressed in both membrane and cytoplasm, and PLCδ3 is expressed in membrane. In our hands, PLCδ1 showed denser fluorescence intensity where TRPC4β is present, and they showed co-localization. Interestingly, PLCδ3 was observed to be empty in the channel puncta region when it was expressed with TRPC4β or TRPC5 (Fig. 1A, C). As PLC is a membrane-associated enzyme and TRPC channels are transmembrane channels, this expression pattern implies that the membrane resident proteins are present on the membrane competitively. Also, this difference presumably reflects that TRPC4β channel has specificity in PLC interaction, and membrane molecules cannot co-exist on the membrane unless they are interacting together.

In this study, we highlight that PLCδ1 binds to TRPC4β but not TRPC5, and it affects PIP_2 level to regulate channel activity. TRPC4 and TRPC5 have a high similarity in amino acid sequence, and thus their structures are almost identical. However, they have some differences in their characteristics. First, TRPC5 shows constitutive activity while TRPC4 does not show channel activity in the absence of stimulation. Second, TRPC4 has a higher affinity for PIP_2 than TRPC5. In a preceding study, TRPC5 showed robust current inhibition with weak voltage stimulation which activates voltage-sensitive phosphatase. Based on our data, we suggest that PIP_2 and PLCδ1 are possible candidates underlying these features [3]. TRPC4β-bound PLCδ1 would continuously regulate PIP_2 level in the vicinity of the channel even without the stimulation, and it would attribute to TRPC4β showing no basal activity. In our hands, TRPC5 interacts with neither PLCδ1 nor PLCδ3, thus relatively abundant PIP_2 pool would exist around TRPC5. The detailed knowledge of mechanism causing differences between TRPC4β and TRPC5 is important in understanding how they differently function physiologically in human body, but it should be elucidated in more detail.

Electrophysiological experiments suggest that PLCδ1 activity produces decreased TRPC4β currents in a calcium dependent manner. In the presence of PLCδ1, EA-evoked TRPC4β currents were significantly reduced (Fig. 3). Whether calcium increase alone causes the optimal activation of PLCδ1 is still controversial. It was suggested that high extracellular potassium, or stimulations like thapsigargin or ionomycin also causes an increase in IP_3, but much less than the amount that is increased by the fully activated PLCδ subtypes [14,15,33]. Through experiments with differing intracellular calcium concentrations, our data agree with the notion that the channel-induced calcium influx within the physiological calcium range is sufficient to activate PLCδ1. In our hands, 50 nM of $[Ca^{2+}]_i$ condition was not enough to fully activate PLCδ1, but PLCδ1 significantly reduced channel currents in higher calcium conditions (100 and 500 nM). Thus, we mainly used 100 nM $[Ca^{2+}]_i$ buffering solution in electrophysiological experiments which showed prominent differences including re-

duced current amplitude and altered time course of currents in the presence of PLCδ1. Interestingly, the time course of channel currents was changed depending on the presence of PLCδ1 (Fig. 3C) or intracellular calcium concentration (Fig. 3E). It is well known that the TRPC4 and TRPC5 channels show desensitization after they are activated by G_qPCR pathway [34-36]. Therefore, such desensitization with PLCδ1 and calcium might also explain the inclusion of PIP_2 in this negative regulation mechanism. Our data showed that the kinetics of the process was much slower with low calcium which has a latency to respond to the channel agonist (Fig. 3). This observation is coincident with the fact that intracellular calcium strongly potentiates TRPC channels [24]. However, this reaction rate was not influenced by the presence of PLCδ1 in the same calcium condition, hence we concluded that when PIP_2 levels are diminished with PLCδ1, equivalent stimulus intensity will be less effective.

By monitoring the PIP_2 level changes after TRPC4β stimulation, we suggest that PLCδ1 accelerates PIP_2 hydrolysis in response to calcium influx (Fig. 4). As a second approach to demonstrate the involvement of PIP_2 in this mechanism, we used PLCδ1 mutant which cannot hydrolyze PIP_2 (Fig. 5). We expected that the PLCδ1-reduced TRPC4β currents might not be observed when PLCδ1 is unable to degrade PIP_2. In electrophysiological experiments, these PLCδ1 mutants did not affect the channel currents. Therefore, it is likely that the PIP_2 is the main source of negative feedback regulation by PLCδ1, and we emphasize the PIP_2 as a requisite component for TRPC4β activation in this negative feedback mechanism of PLC.

Until now, we only focused on PIP_2 as an indispensable component for TRPC4 channel activity, and the channel seems to fall into desensitization when PIP_2 level is decreased. It should be noted that other groups have proposed the inhibitory effect of PIP_2 on TRPC4 [6,37]. Recent evidence suggests that PIP_2 has a dual regulatory role, and yet it remains an open question as to how PIP_2 decides its role. TRPV1 has also been proposed to be regulated by PIP_2 with a duality in function. Initially, TRPV1 channel was suggested to be potentiated after PIP_2 hydrolysis by releasing inhibitory PIP_2 from the channel [18,38-40].

Previously, it is suggested that the activity of PLCδ1 does not exhibit receptor-specific activation [41]. In the electrophysiological experiments, we used channel-specific and strong agonist, hence we suggest that PLCδ1 is activated by channel-mediated calcium. However, it is still obscure how EA is involved in the signaling pathway that activates TRPC4β. The other group specified that PLCδ1 is involved in the $G\alpha_{i/o}$-mediated TRPC4 activation. It should be elucidated whether the activation of PLCδ1 is confined to the specific pathway or the calcium through the channel itself is enough.

Collectively, our data reveal that TRPC4β-interacting PLCδ1 is sensitively activated by the calcium influx through TRPC4β and in turn, hydrolyzes TRPC4β-PI(4,5)P_2 which maintains TRPC4β activity. Consequently, PLCδ1 is a negative regulator of TRPC4β.

FUNDING

This work was supported by the National Research Foundation of Korea (NRF) grants funded by the Korean government (2020R1A2C1012670, 2021R1A4A2001857) (I.S.) and the Education and Research Encouragement Fund of Seoul National University Hospital (I.S.). J. Kim. was supported by the BK21 program from the Ministry of Education.

ACKNOWLEDGEMENTS

We thank Jung Eun Lee (Seoul National University, Seoul, Korea) and Christine Haewon Park (Seoul National University, Seoul, Korea) for helpful discussion and proofreading of manuscript. Careful proofreading was done by native speakers of English.

CONFLICTS OF INTEREST

The authors declare no conflicts of interest.

SUPPLEMENTARY MATERIALS

Supplementary data including two figures can be found with this article online at https://doi.org/10.4196/kjpp.2023.27.2.187.

REFERENCES

1. Kim BJ, Kim MT, Jeon JH, Kim SJ, So I. Involvement of phosphatidylinositol 4,5-bisphosphate in the desensitization of canonical transient receptor potential 5. *Biol Pharm Bull.* 2008;31:1733-1738.
2. Kim H, Jeon JP, Hong C, Kim J, Myeong J, Jeon JH, So I. An essential role of PI(4,5)P_2 for maintaining the activity of the transient receptor potential canonical (TRPC)4β. *Pflugers Arch.* 2013;465:1011-1021.
3. Ko J, Myeong J, Shin YC, So I. Differential PI(4,5)P_2 sensitivities of TRPC4, C5 homomeric and TRPC1/4, C1/5 heteromeric channels. *Sci Rep.* 2019;9:1849.
4. Otsuguro K, Tang J, Tang Y, Xiao R, Freichel M, Tsvilovskyy V, Ito S, Flockerzi V, Zhu MX, Zholos AV. Isoform-specific inhibition of TRPC4 channel by phosphatidylinositol 4,5-bisphosphate. *J Biol Chem.* 2008;283:10026-10036.
5. Mederos Y Schnitzler M, Gudermann T, Storch U. Emerging roles of diacylglycerol-sensitive TRPC4/5 channels. *Cells.* 2018;7:218.
6. Storch U, Forst AL, Pardatscher F, Erdogmus S, Philipp M, Gregoritza M, Mederos Y Schnitzler M, Gudermann T. Dynamic NHERF interaction with TRPC4/5 proteins is required for channel gating by diacylglycerol. *Proc Natl Acad Sci U S A.* 2017;114:E37-E46.
7. Zhu MH, Chae M, Kim HJ, Lee YM, Kim MJ, Jin NG, Yang DK, So I, Kim KW. Desensitization of canonical transient receptor po-

tential channel 5 by protein kinase C. *Am J Physiol Cell Physiol.* 2005;289:C591-C600.
8. Myeong J, Ko J, Kwak M, Kim J, Woo J, Ha K, Hong C, Yang D, Kim HJ, Jeon JH, So I. Dual action of the Gαq-PLCβ-PI(4,5)P_2 pathway on TRPC1/4 and TRPC1/5 heterotetramers. *Sci Rep.* 2018;8:12117.
9. Ko J, Myeong J, Kwak M, Jeon JH, So I. Identification of phospholipase C β downstream effect on transient receptor potential canonical 1/4, transient receptor potential canonical 1/5 channels. *Korean J Physiol Pharmacol.* 2019;23:357-366.
10. Berridge MJ. Inositol trisphosphate and calcium signalling. *Nature.* 1993;361:315-325.
11. Noh DY, Shin SH, Rhee SG. Phosphoinositide-specific phospholipase C and mitogenic signaling. *Biochim Biophys Acta.* 1995;1242:99-113.
12. Rhee SG, Choi KD. Regulation of inositol phospholipid-specific phospholipase C isozymes. *J Biol Chem.* 1992;267:12393-12396.
13. Lee SB, Rhee SG. Significance of PIP2 hydrolysis and regulation of phospholipase C isozymes. *Curr Opin Cell Biol.* 1995;7:183-189.
14. Kim YH, Park TJ, Lee YH, Baek KJ, Suh PG, Ryu SH, Kim KT. Phospholipase C-delta1 is activated by capacitative calcium entry that follows phospholipase C-beta activation upon bradykinin stimulation. *J Biol Chem.* 1999;274:26127-26134.
15. Allen V, Swigart P, Cheung R, Cockcroft S, Katan M. Regulation of inositol lipid-specific phospholipase cdelta by changes in Ca^{2+} ion concentrations. *Biochem J.* 1997;327(Pt 2):545-552.
16. Rebecchi MJ, Pentyala SN. Structure, function, and control of phosphoinositide-specific phospholipase C. *Physiol Rev.* 2000;80:1291-1335.
17. Cifuentes ME, Delaney T, Rebecchi MJ. D-myo-inositol 1,4,5-trisphosphate inhibits binding of phospholipase C-delta 1 to bilayer membranes. *J Biol Chem.* 1994;269:1945-1948.
18. Lukacs V, Thyagarajan B, Varnai P, Balla A, Balla T, Rohacs T. Dual regulation of TRPV1 by phosphoinositides. *J Neurosci.* 2007;27:7070-7080.
19. Rohács T, Lopes CM, Michailidis I, Logothetis DE. PI(4,5)P_2 regulates the activation and desensitization of TRPM8 channels through the TRP domain. *Nat Neurosci.* 2005;8:626-634.
20. Erickson MG, Alseikhan BA, Peterson BZ, Yue DT. Preassociation of calmodulin with voltage-gated Ca^{2+} channels revealed by FRET in single living cells. *Neuron.* 2001;31:973-985.
21. Epe B, Steinhäuser KG, Woolley P. Theory of measurement of Förster-type energy transfer in macromolecules. *Proc Natl Acad Sci U S A.* 1983;80:2579-2583.
22. Patterson G, Day RN, Piston D. Fluorescent protein spectra. *J Cell Sci.* 2001;114(Pt 5):837-838.
23. Kwak M, Hong C, Myeong J, Park EYJ, Jeon JH, So I. $G\alpha_i$-mediated TRPC4 activation by polycystin-1 contributes to endothelial function via STAT1 activation. *Sci Rep.* 2018;8:3480.
24. Blair NT, Kaczmarek JS, Clapham DE. Intracellular calcium strongly potentiates agonist-activated TRPC5 channels. *J Gen Physiol.* 2009;133:525-546.
25. Garcia P, Gupta R, Shah S, Morris AJ, Rudge SA, Scarlata S, Petrova V, McLaughlin S, Rebecchi MJ. The pleckstrin homology domain of phospholipase C-delta 1 binds with high affinity to phosphatidylinositol 4,5-bisphosphate in bilayer membranes. *Biochemistry.* 1995;34:16228-16234.
26. Ellis MV, U S, Katan M. Mutations within a highly conserved sequence present in the X region of phosphoinositide-specific phospholipase C-delta 1. *Biochem J.* 1995;307(Pt 1):69-75.
27. Zhang Z, Okawa H, Wang Y, Liman ER. Phosphatidylinositol 4,5-bisphosphate rescues TRPM4 channels from desensitization. *J Biol Chem.* 2005;280:39185-39192.
28. Liu D, Liman ER. Intracellular Ca^{2+} and the phospholipid PIP_2 regulate the taste transduction ion channel TRPM5. *Proc Natl Acad Sci U S A.* 2003;100:15160-15165.
29. Liu B, Qin F. Functional control of cold- and menthol-sensitive TRPM8 ion channels by phosphatidylinositol 4,5-bisphosphate. *J Neurosci.* 2005;25:1674-1681.
30. Daniels RL, Takashima Y, McKemy DD. Activity of the neuronal cold sensor TRPM8 is regulated by phospholipase C via the phospholipid phosphoinositol 4,5-bisphosphate. *J Biol Chem.* 2009;284:1570-1582.
31. Yudin Y, Lutz B, Tao YX, Rohacs T. Phospholipase C δ4 regulates cold sensitivity in mice. *J Physiol.* 2016;594:3609-3628.
32. Lukacs V, Yudin Y, Hammond GR, Sharma E, Fukami K, Rohacs T. Distinctive changes in plasma membrane phosphoinositides underlie differential regulation of TRPV1 in nociceptive neurons. *J Neurosci.* 2013;33:11451-11463.
33. Banno Y, Okano Y, Nozawa Y. Thrombin-mediated phosphoinositide hydrolysis in Chinese hamster ovary cells overexpressing phospholipase C-delta 1. *J Biol Chem.* 1994;269:15846-15852.
34. Tsvilovskyy VV, Zholos AV, Aberle T, Philipp SE, Dietrich A, Zhu MX, Birnbaumer L, Freichel M, Flockerzi V. Deletion of TRPC4 and TRPC6 in mice impairs smooth muscle contraction and intestinal motility in vivo. *Gastroenterology.* 2009;137:1415-1424.
35. Dresviannikov AV, Bolton TB, Zholos AV. Muscarinic receptor-activated cationic channels in murine ileal myocytes. *Br J Pharmacol.* 2006;149:179-187.
36. Lee KP, Jun JY, Chang IY, Suh SH, So I, Kim KW. TRPC4 is an essential component of the nonselective cation channel activated by muscarinic stimulation in mouse visceral smooth muscle cells. *Mol Cells.* 2005;20:435-441.
37. Thakur DP, Tian JB, Jeon J, Xiong J, Huang Y, Flockerzi V, Zhu MX. Critical roles of Gi/o proteins and phospholipase C-δ1 in the activation of receptor-operated TRPC4 channels. *Proc Natl Acad Sci U S A.* 2016;113:1092-1097.
38. Klein RM, Ufret-Vincenty CA, Hua L, Gordon SE. Determinants of molecular specificity in phosphoinositide regulation. Phosphatidylinositol (4,5)-bisphosphate (PI(4,5)P_2) is the endogenous lipid regulating TRPV1. *J Biol Chem.* 2008;283:26208-26216.
39. Liu B, Zhang C, Qin F. Functional recovery from desensitization of vanilloid receptor TRPV1 requires resynthesis of phosphatidylinositol 4,5-bisphosphate. *J Neurosci.* 2005;25:4835-4843.
40. Rohacs T, Thyagarajan B, Lukacs V. Phospholipase C mediated modulation of TRPV1 channels. *Mol Neurobiol.* 2008;37:153-163.
41. Murthy SN, Lomasney JW, Mak EC, Lorand L. Interactions of G(h)/transglutaminase with phospholipase Cdelta1 and with GTP. *Proc Natl Acad Sci U S A.* 1999;96:11815-11819.